Estimating The Effects of Ocean Acidification on Coastal Communities: A Case Study in South Puget Sound

Om Nerurkar Teacher/Mentor: Mr. Gotwals / Dr. Murray and Dr. Waldbusser Research in Computational Science North Carolina School of Science and Math 12 November 2020

#### Acknowledgement

I would like to acknowledge Dr. James W. Murray and Dr. George Waldbusser for helping me gain a deeper understanding of both geochemistry and biological response factors. Dr. Murray provided a few chapters from his yet unpublished book on aquatic carbonate chemistry, allowing me to gain an inside look on the physical dynamics underlying ocean acidification. He also guided me on the relationships between key variables that were significant to generating accurate calculations. Dr. Waldbusser aided me in understanding the biological responses of shellfish to such environmental changes, especially the relationship between life stage survival rates and marine chemistry changes.

#### Abstract

South Puget Sound has a thriving shellfish industry that contributes tens of millions of dollars to the Washington State economy and thousands of commercial and recreational jobs. Unfortunately, ocean acidification has begun threatening the viable yield of critical shellfish species in this region, with a documented increase in shellfish die-off events and larval mortality over the past two decades. There is a strong correlation between acidification and global and regional increases in dissolved  $CO_2$  levels. The goal of this study is to predict how changing marine and atmospheric  $CO_2$  levels will affect the yield rates of the two most economically valuable farmed shellfish species in Washington State, and how changing yield rates will affect the South Puget Sound bay community. This study utilizes systems-dynamics modeling to relate included variables in three main phases. The first phase is an aquatic chemistry model that relates fluctuating  $CO_2$  levels to a saturation rate. The second phase relates the changing calcium carbonate saturation rate and pH to the shellfish yield rates of two species. The third phase then estimates consequent effects on the local South Puget Sound economy. The conclusions derived from this study support future research on the effects of ocean acidification and other forms of climate change on aquaculture yield and regional economic development. They identify variables significant to economic and environmental health, as well as policy and technology-based solutions to the consequences of acidification.

# Contents

1.	roduction	4					
2.	Con	nputational Approach/Methods	6				
	2.1	STELLA Architect	6				
	2.2	LoggerPro	7				
	2.3	Aquatic Chemistry and Carbon Dynamics	8				
	2.4	Population Dynamics	10				
	2.5	Economical Dynamics Models	11				
3.	Res	cults	13				
	3.1	Aquatic Chemistry Model	13				
	3.2	Population Dynamics Models	14				
	3.3	Economical Dynamics Models	15				
4.	4. Discussion and Conclusion						
	4.1	Aquatic Chemistry Model	17				
	4.2	Population Dynamics Models	18				
	4.3	Economical Dynamics Models	18				
	4.4	Model Limitations and Future Research	19				
	4.5	Potential Solutions					
	4.6	Final Conclusion					

#### 1. Introduction

Ocean acidification (OA) is a phenomenon that occurs when marine waters experience an increase in dissolved CO<sub>2</sub> levels (Pacella et. al., 2018). In South Puget Sound, Washington State, changes in estuarine water chemistry due to ocean acidification are especially notable due to the upwelling of  $CO_2$  rich water from the Pacific (Feely et. al., 2008) (Alin et. al., 2010). These changes in aquatic geochemistry threaten all marine life, but negatively affect calcifying organisms in particular (Bressnan et. al., 2014). Many calcifying organisms, including corals, crustaceans, echinoderms, and molluscs, secrete aragonite to build their shells. Ocean acidification impedes this process, with previous studies demonstrating a high correlation between aragonite saturation state  $\Omega_{arag}$  and hatchery failures (Barton et. al., 2015). Lowered  $\Omega_{arag}$  forces shellfish to expend more energy in shell production, often leading to deformation and lowered population values (Timmins-Schiffman et. al., 2019). Bivalve shellfish in Washington State have experienced some of the worst effects of ocean acidification. In 2007, the Whiskey Creek Shellfish Company experienced a severe mortality event that devastated local shellfish larvae populations, resulting in net zero profit for major production companies in the region (Schreiber, 2018). This event coincided with abnormal upwelling rates in the Pacific Northwest over a two year period. In 2014, a study conducted by Oregon State University determined that 50% of those in the West Coast shellfish industry have directly observed the effects of ocean acidification, while 75% claimed to be worried about OA (Mabardy, 2014). Northwestern tribal fisheries have also experienced mortality events correlated with increases in regional upwelling, an example of how OA threatens ways of life intrinsically connected to natural resources (U.S. Climate Resilience). Regional shellfish aquaculture is a key industry in Washington State, contributing over \$50 million annually to the South Puget Sound economy alone (Washington State Legislature, 2015). This study aimed to predict how changing  $CO_2$  levels in both the atmosphere and deep ocean will affect shellfish populations. It also estimated the economic viability of the South Puget Sound shellfish industry and the regional job market. Utilizing a three-step systems-dynamics model, this study illustrated how changes in marine geochemistry will adversely affect the South Puget Sound community.

The majority of dissolved CO2 absorbed from the atmosphere remains within the epipelagic and upper mesopelagic zones of the ocean (Feely, 2008). Therefore, it was important to study the upper 400 meter surface ocean to determine the most significant impacts of ocean acidification. Since these regions are close to the marine surface, atmospheric-marine  $CO_2$  flux (the  $CO_2$  exchange rate between the ocean and atmosphere) is important to estimate, especially as atmospheric  $CO_2$  levels rise due to human-caused (anthropogenic) emissions. The  $CO_2$  concentration of the upwelled water is also significant, as there is a difference between the rate at which surface and deep water reflect atmospheric  $CO_2$  levels. Therefore, seasonal and annual upwelling rates must be considered separately from atmospheric-marine flux (Feely et. al., 2010). The South Puget Sound region has a special case of ocean acidification, with marine  $pCO_2$  levels already being higher than atmospheric  $pCO_2$  values (Bush et. al., 2013). In 2000, the Intergovernmental Panel for Climate Change (IPCC) generated  $CO_2$  prediction models for numerous climate scenarios. The

A1F1 scenario, also known as the "fossil fuel intensive" scenario, predicts how atmospheric  $CO_2$  levels will change over the 21st century (IPCC, 2000). To illustrate the potential effects of ocean acidification, I used this scenario in the  $CO_2$  dynamics model. Atmospheric  $CO_2$  levels fluctuate on a seasonal basis, as observed by Keeling Curve data. In the Northern Hemisphere, plant decomposition over the fall and winter months results in a net increase in atmospheric  $CO_2$  peaking in May (Monroe, 2013). Over the spring and summer months, plant growth reverses this cycle. To account for seasonal accumulation, the Keeling Curve was integrated with the A1F1  $CO_2$  prediction curve.

Increases in marine surface  $pCO_2$  have significant effects on other geochemical factors. When dissolved  $CO_2$  levels increase, a series of chemical reactions decrease seawater pH as well as the carbonate ion concentration  $(CO_3^{2-})$ . Decreases in  $CO_3^{2-}$  concentration affect the saturation states of inorganic minerals such as aragonite  $(\Omega_{arag})$  and calcite  $(\Omega_{cal})$ , both forms of calcium carbonate  $(CaCO_3)$  (Feely et. al., 2010). While the causes of ocean acidification are numerous, global increases in anthropogenic  $CO_2$  concentrations have been directly correlated with increases in the partial pressure of seawater  $CO_2$  ( $pCO_{2SWS}$ ) (Doney, 2009).  $pCO_2$  is a measure of the gaseous pressure in equilibrium with a given dissolved  $CO_2$  level. To estimate changes in pH and  $\Omega_{arag}$  in South Puget Sound due to ocean acidification, I considered other variables. I related pH to Alkalinity,  $pCO_2$ , and the dissociation constants  $K_1$ ,  $K_2$ , and  $K_H$ . These dissociation constants measure the ability of larger components in a mixture to dissociate, or break down into smaller components (Murray). Alkalinity is a measure of how easily a body of water can resist changes in pH, and also varies based on salinity (Fassbender, 2016). Salinity is the measure of dissolved salt, or the 11 major ion concentrations in seawater. Aragonite saturation state  $(\Omega_{arag})$  was calculated from the Ion Concentration Product (ICP) and the aragonite dissociation constant  $(K_1S_{0arag})$  (Murray). ICP is the sum measure of separate ion concentrations.  $K_1S_{0arag}$  measures how easily aragonite can dissociate. Other significant values include Dissolved Inorganic Carbon (DIC) and Carbon Alkalinity ( $C_{Alk}$ ). DIC is the total measure of  $CO_2$ dissolved in a body of water, while  $C_{Alk}$  is a measure of alkalinity without a borate  $(BO_3^{3-})$  component (Murray). As marine  $pCO_2$  levels rise, we can expect that both pH and  $\Omega_{arag}$  will drop as well (Feely et. al., 2010). Although we could have used pH to reasonably predict the effects of ocean acidification on marine organisms, a slight decoupling occurs between  $\Omega_{arag}$  and pH when the time interval  $\Delta t$  is increased. For the purpose of accuracy in this 80-year model, we took extra steps to calculate  $\Omega_{arag}$  in addition to pH.

The two most economically valuable shellfish species in the South Puget Sound region are the Geoduck (Panopea Generosa) and the Pacific Oyster (Crassostrea Gigas). In 2013, the Geoduck accounted for 44% of South Puget Sound's shellfish production value, or approximately \$23.7 million. That same year, the Pacific Oyster accounted for 22% of South Puget Sound's shellfish production value, or approximately \$11.4 million (Washington State Legislature, 2015). These figures only take into consideration commercial production values. The economic value produced by recreational farming is difficult to estimate, but it is widely agreed that commercial production value is significantly larger (Barton et. al., 2015). In 2013, recreational geoduck farming contributed \$3.6 million to the South Puget Sound economy (Washington).

This study will focus on commercial production values and assume recreational production values to be negligible. It is also important to note the primary methods through which Geoducks and Pacific Oysters harvests happen. Geoducks often spend the majority of their life cycle in the wild, with harvests occurring once they attain market-size (approx. 2.07 lbs) in a 3-year period (Washington). Their habitat in the shallow South Puget Sound coast leaves Geoducks exposed to ocean acidification from the larval stage through harvesting. Pacific Oysters spend their larval stage in controlled hatcheries, but are post-larvally grown from aquaculture tanks that are often exposed to South Puget Sound's waters (Food and Agriculture). They harvest at market size (approx. 0.154 lbs) in 18 to 30 months (Food and Agriculture). A significant assumption is that both Geoducks and Pacific Oysters reproduce before harvesting, which is not always the case. Since Geoducks exposure to acidic water occurs in the larval stage, while it does not for Pacific Oysters, we used different computational approaches in relating seawater chemistry changes to each species' development rate. The relationship between  $\Omega_{arag}$  and shellfish birth and mortality rates has not been extensively studied. However, the relationship between  $\Omega_{arag}$  and certain species' growth rates at the larval stage has been reasonably established (Timmins-Schiffman et. al., 2019).

We used six values to analyze economic behavior directly caused by ocean acidification in South Puget Sound. We calculated the net income and the net profit from both species from initial values from 2013, and assumed the value per pound to be constant. The net profit per pound was also assumed to be a constant (Washington State Legislature, 2015). Net income and net profit loss change are significant since they illustrate lasting economic impacts beyond instantaneous financial loss. The impacts of income and profit loss on the South Puget Sound community are various, including potential widening of current socioeconomic gaps (Lemonick, 2012). For the purposes of this study, we only studied jobs directly related to the shellfish industry.

### 2. Computational Approach/Methods

#### 2.1 STELLA Architect

STELLA Architect is a systems-dynamics modeling tool. It allows the user to model complex systems through time-series simulations and variable relationships. "Stocks" are variables that accumulate values over time. I utilized stocks for parameters that required system memory. They are dependent on "flows," or rates of material transfer from outside the model to stocks and transfer between stocks. "Converters," or parameters not requiring system memory, can either be factors into flow rates, be independent variables, or be dependent on external values (Ford, 2010).

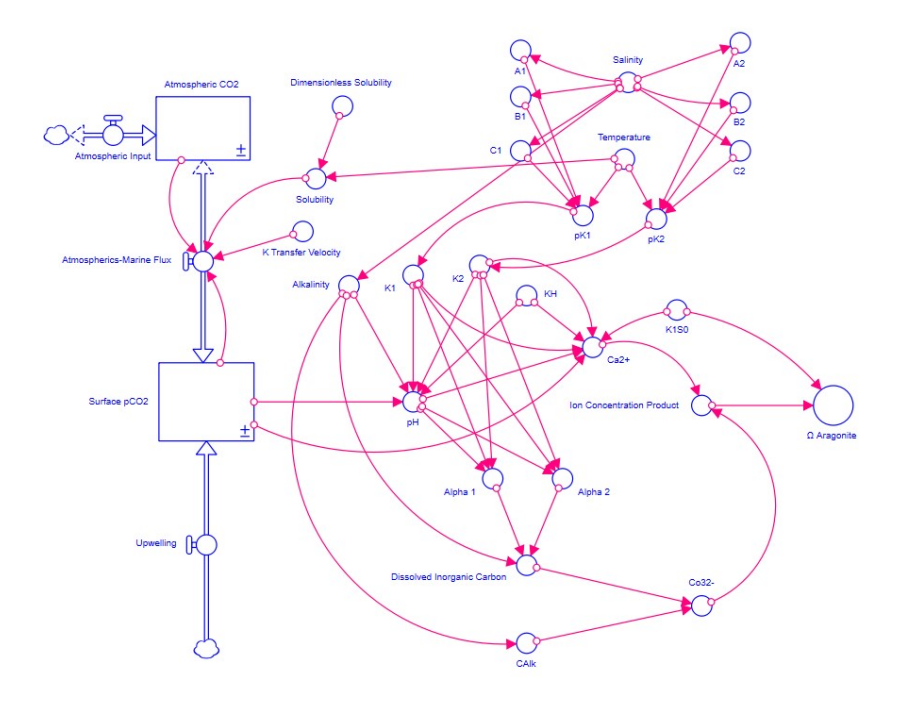


Figure 1: Aquatic Chemistry Sector

I split the systems model into three primary sectors. The first sector is an aquatic chemistry model that relates atmospheric-marine  $pCO_2$  values and upwelling rates in SPS to changes in  $\Omega_{arag}$  and pH. The second sector calculates biological response and population changes for both shellfish species from changes in  $\Omega_{arag}$  and pH. The third sector then predicts the changes in net communal income and economic consequences for the SPS community. I optimized the model parameters for convenience. To account for accuracy in the 80-year predictions, the model has a monthly time step. I utilized a  $\Delta t$  of 12 months to calculate annual economic estimates.

### 2.2 LoggerPro

LoggerPro is a data-analysis tool that produces regression fits. We used LoggerPro to produce both the atmospheric  $CO_2$  input and upwelling rate functions. It was also utilized in the production of numerous shellfish biological response functions related to growth rates.

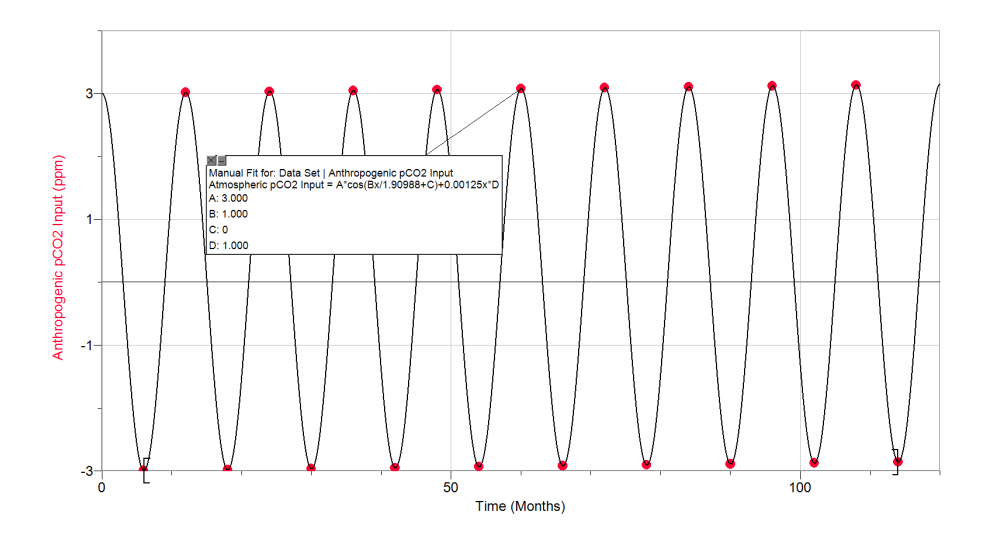


Figure 2: Increasing Anthropogenic Atmospheric  $CO_2$  Input Model

### 2.3 Aquatic Chemistry and Carbon Dynamics

The study site for this model was South Puget Sound (SPS), WA (47° 36′ 0.00″ N, 122° 27′ 0.00″ W). The models runs for 960 months, ending on July 1st, 2100 from a starting date in July 1st, 2020. I assumed initial surface  $pCO_2$  (560 ppm) and initial atmospheric  $pCO_2$  (420 ppm) values from the Global Ocean Acidification Observing Network Dabob Bay Buoy (GOA Explorer). Dabob Bay is part of a subcanal geographically close to Puget Sound, and shares similar upwelling and atmospheric-marine exchange processes to SPS (PMEL Carbon Program). I averaged the minimum (278.7° Kelvin) and maximum (298° Kelvin) observed temperatures in Dabob Bay and assumed a constant surface temperature of 288.35° Kelvin. The sinusoidal function we generated mimics seasonal fluctuations of 5° Kelvin in Dabob Bay utilizing LoggerPro software.

I assumed a constant salinity of 30 ppt (parts per thousand) from data in Dabob Bay. To calculate alkalinity, I used the equation (47.7\*Salinity) + 647 (Estimating Total Alkalinity). This yielded a constant value of 2078  $\mu mol~kg^{-1}$ . I then generated a sinusoidal function matching seasonal peaks from Dabob Bay to mimic industrial atmospheric  $CO_2$  input. The subsequent atmospheric  $pCO_2$  values matched the IPCC's A1F1 atmospheric carbon scenario. To account for seasonal accumulation, we integrated Keeling Curve data with the A1F1  $CO_2$  prediction curve.

I utilized the equation  $Flux = K_w K_0(\Delta p CO_2)$  to calculate atmospheric-marine flux per unit area (Wanninkhof, 1999). This equation estimates diffusion rates across a fixed boundary layer (in this case the marine surface). This relationship is represented in the model by a biflow, meaning that  $CO_2$  exchange can happen in either direction between the atmosphere and surface ocean.  $K_w$  is the k-transfer velocity,  $K_0$  is the solubility, and  $\Delta p CO_2$  is the net difference in  $p CO_2$  values in SPS and the atmosphere. Based on average wind speeds in SPS (Wanninkhof, 1999), I assumed  $K_w$  to be a constant. I then calculated  $K_0$  using the below function (in  $\mu mol$ ) (Wanninkhof, 1999).

$$Ca2+ = (Dimensionless\ Solubility/(8.3145*Temperature))/10$$

I assumed dimensionless solubility to be 1  $mol\ l^{-1}$  (Weiss, 1974). To develop an upwelling rate of  $pCO_2$ , I used the difference in atmospheric  $pCO_2$  inputs and peak predicted marine  $pCO_2$  values in Dabob Bay (GOA Explorer). The difference function generated the below sinusoidal fit equation.

$$Upwelling = 0.1 * cos(Time/1.90988) + (0.0001 * Time) + 0.1)$$

The solubility product  $K_H$  was assumed to be  $10^{-1.53} \ molkg^{-1}atm^{-1}$ , chosen relative to a temperature of 298° Kelvin and a salinity of 35 ppt. This value does not fluctuate extensively (Murray), so I held it as a constant. I then calculated the disassociation constants  $K_1$  and  $K_2$  from the negative base ten logarithmic functions ( $pK_1$  and  $pK_2$ ) of temperature and salinity. I assumed  $K_1S_0$  to be  $6.46 * 10^{-7}$  (Murray). Seawater scale ( $pK_{SWS}$ ) regression values determined  $pK_1$  and  $pK_2$ .

Table 1. Coefficients for the fits of the values of  $pK_1$  in seawater as a function of temperature, salinity and ionic strength on the  $pH_F$ ,  $pH_T$  and  $pK_{SWS}$  scales

		pH <sub>F</sub> scale	pH <sub>T</sub> scale	pH <sub>SWS</sub> scale
S <sup>0.5</sup>	a <sub>0</sub>	5.09247	13.4051	13.4038
S	$a_1$	0.05574	0.03185	0.03206
$S^2$	$a_2$	-9.279E-05	-5.218E-05	-5.242E-05
$S^{0.5}/T$	a <sub>3</sub>	-189.879	-531.095	-530.659
S/T	a <sub>4</sub>	-11.3108	-5.7789	-5.8210
S <sup>0.5</sup> ln T	as	-0.8080	-2.0663	-2.0664
s.e.		0.0055	0.0053	0.0053
Number		551	551	551

Figure 3: Seawater Scale Regression Values (Murray)

The below six equations were used to calculate  $pK_1$  and  $pK_2$ . Equations 17-18 were added to the function of regression constants and temperature.

$$\begin{split} pK_1^0 &= -126.34048 + 6320.813/T + 19.568224 \ln T & (17) \\ pK_2^0 &= -90.18333 + 5143.692/T + 14.613358 \ln T & (18) \\ A_i &= a_0 S^{0.5} + a_1 S + a_2 S^2 & (19) \\ B_i &= a_3 S^{0.5} + a_4 S & (20) \\ C_i &= a_5 S^{0.5} & (21) \\ pK_i - pK_i^0 &= A_i + B_i/T + C_i \ln T \end{split}$$

Figure 4: Disassociation Equations (Murray)

Surface pH was calculated as a function of Surface  $pCO_2$ ,  $K_H$ ,  $K_1$ ,  $K_2$ , and Alkalinity (Murray).

$$(H^{+}) = \left\{ -K_{1}' \left( Alk - C_{T} \right) + \left[ (K_{1}')^{2} \left( Alk - C_{T} \right)^{2} - 4 \ Alk \ K_{1}' \ K_{2}' \left( Alk - C_{T} \right) \right] \right\} / \ 2 \ Alk \ K_{1}' \ K_{2}' \left( Alk - C_{T} \right) \right] + \left[ (K_{1}')^{2} \left( Alk - C_{T} \right)^{2} - 4 \ Alk \ K_{1}' \ K_{2}' \left( Alk - C_{T} \right) \right] + \left[ (K_{1}')^{2} \left( Alk - C_{T} \right)^{2} - 4 \ Alk \ K_{1}' \ K_{2}' \left( Alk - C_{T} \right) \right] \right\} / \ 2 \ Alk \ K_{1}' \ K_{2}' \left( Alk - C_{T} \right) + \left[ (K_{1}')^{2} \left( Alk - C_{T} \right)^{2} - 4 \ Alk \ K_{1}' \ K_{2}' \left( Alk - C_{T} \right) \right] + \left[ (K_{1}')^{2} \left( Al$$

ICP was developed as a function of carbonate  $(CO_3^{2-})$  and the calcium cation  $(Ca^{2+})$ .  $Ca^{2+}$  was estimated using the below equation.

$$(K_{1S}0 * K_1 * K_2)/(K_H * (pCO_2/1000000) * (10^{-pH}))$$

 $CO_3^{2-}$  was assumed to be the absolute difference between  $C_{Alk}$  and DIC (Murray). I assumed  $C_{Alk}$  to be 97.7% of Alkalinity to account for borate (Gast et. at., 1958). DIC was calculated as a function of Alkalinity,  $\alpha_1$  and  $\alpha_2$  (dimensionless values). I derived  $\Omega_{arag}$  from ICP and  $K_1S0$ .

# 2.4 Population Dynamics

Due to the lack of experimental data, it was necessary to convert the mathematical relationship between  $\Omega_{arag}$  and each species' growth rates to a relationship between  $\Omega_{arag}$  and each species' birth rates. pH and  $\Omega_{arag}$  affect each species at different rates during different life stages, with the larval stage being the most vulnerable (Timmins-Schiffman et. al., 2019). To account for this, I constructed both the Pacific Oyster and Geoduck population models in a step-based format, with each "stock" representing an age group. The Pacific Oyster model measured the larval stage population value and the net harvest weight in South Puget Sound. The Geoduck model also measured the larval stage population value and the net harvest weight in South Puget Sound. To account for stunted larval grow, I added a dissoconch stage (immediately post-larvae). I neglected mortality rate changes due to acidification, deeming them relatively insignificant to the population feedback loop, and due to the experimental relationship between  $\Omega_{arag}$  and shellfish mortality being practically nonexistent.

Pacific Oyster birth and mortality rates were therefore held constant. I assumed the mortality rate to be 1/360, as Pacific Oysters live approximately 360 months (Sea Grant). I calculated the birth rate as a function of harvest weight and a constant birth coefficient. I approximated the number of fertile oysters through harvest weight. Due to the lack of experimental data, I assumed a constant  $\Omega_{arag}$  value to calculate the birth coefficient. The relationship between  $\Omega_{arag}$  and C. Gigas mid-stage growth has already been studied (Barton et. al). We converted this relationship to a development rate by utilizing a regression function.

Geoduck birth and early development rates were also held constant. The mortality rate is a constant of 1/1407, given that Geoducks live approximately 1407 months (Alaska). The birth rate was again calculated as a function of harvest weight and a constant birth coefficient. Only the relationship between pH and P. Generosa larvae growth has been previously studied (Timmins-Schiffman et. al., 2019). The lack of experimental data forced us to hold the d-hinge stage developmental rate as a constant. We calculated the dissoconch stage developmental rate by developing regressions matching pH to experimental growth changes.

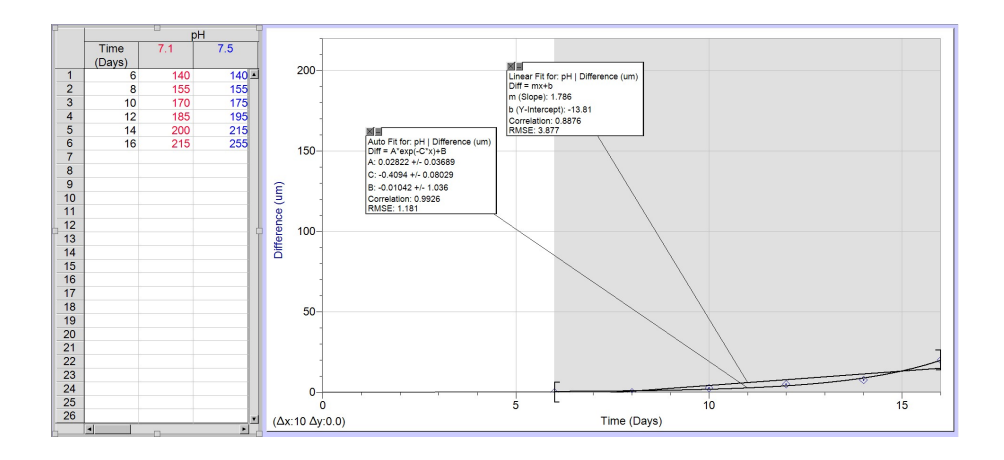


Figure 5: Geoduck Larvae Diameter Difference vs. Time

Figure 5 displays a linear fit (not used) and a quadratic fit (used) in larval diameter differences for different pH values. pH differed by 0.4 points in the study, so each growth rate difference was divided by two on an iterating basis.

### 2.5 Economical Dynamics Models

I calculated net profit from the Pacific Oyster yield as a product of the price per pound value constant and the harvest weight. Assuming a value constant of \$1.08 per pound (Washington State Legislature, 2015), I calculated net profit loss as the difference between constant annual yields and predicted yields. I based constant annual yields on the initial yield. The below integral calculated the accumulation of predicted yields. I then divided net profit by the number of years for annual accumulation.

$$\int_0^t (Net\ Profit)/(Number\ of\ Years)\ dt$$

The net income was also calculated as a product of a value constant and the harvest weight. Taking a value constant of \$15.03 per pound (Washington State Legislature, 2015). Net income loss was again calculated from as the difference between constant annual yields and predicted yields.

I measured job availability for shellfish farmers in South Puget Sound in both proportion of jobs lost and the number at any given time. I also measured the percentage of jobs lost as the difference from initial, assuming the number of jobs correlated directly with net income for both harvests, I generated the below regression fits from net income to calculate the number of jobs.

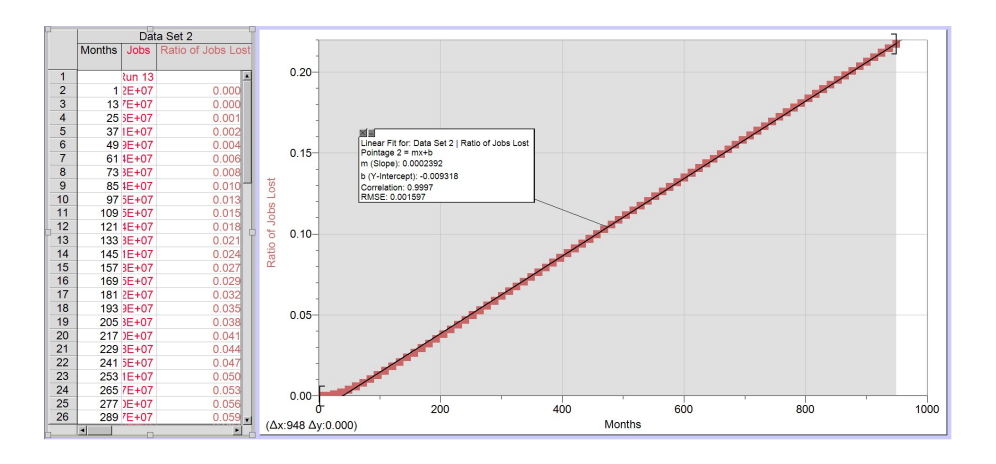


Figure 6: Ratio of Pacific Oyster Harvesting Jobs Lost vs. Time

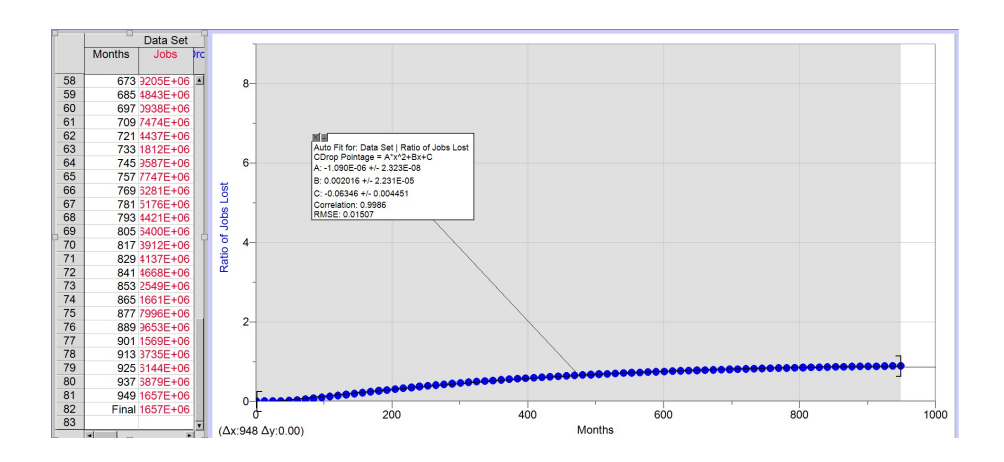
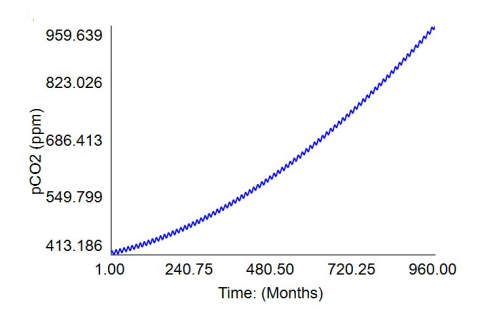


Figure 7: Ratio of Geoduck Harvesting Jobs Lost vs. Time

Figure 6 displays the ratio function of C. Gigas harvesting jobs lost in the South Puget Sound Region. Figure 7 displays the ratio function of P. Generosa harvesting jobs lost in the South Puget Sound Region.

### 3. Results

### 3.1 Aquatic Chemistry Model



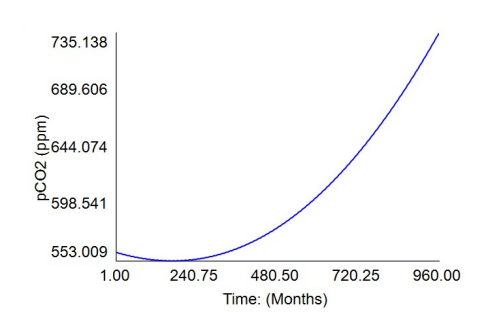
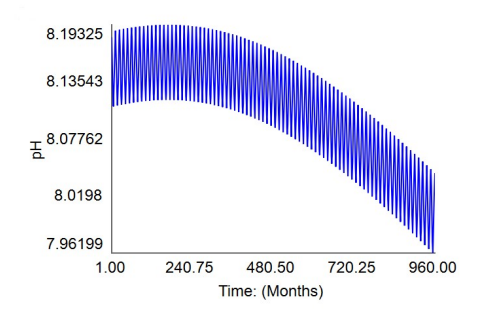


Figure 8: Atmospheric  $pCO_2$ 

Figure 9: Surface  $pCO_2$ 

Comparison of environmental  $pCO_2$  values (ppm) over a time series (Months). Figure 8 represents atmospheric  $pCO_2$  values, Figure 9 represents marine surface  $pCO_2$  values. Seasonal  $pCO_2$  was assumed to peak in May and trough in November for both environments based on the Keeling Curve.



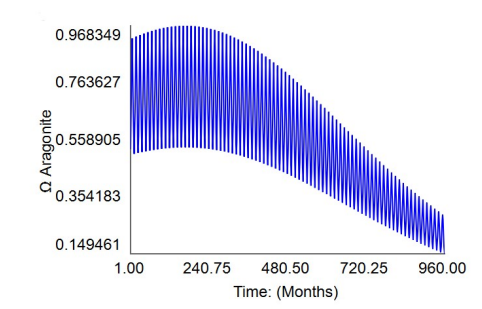
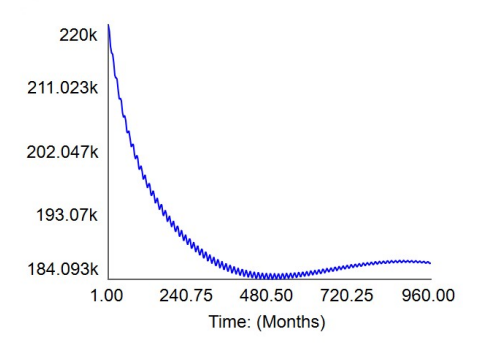


Figure 10: pH

Figure 11: Aragonite Saturation State

Comparison of pH (SWS scale) with  $\Omega_{arag}$ . Both values fluctuate on a seasonal basis, with a peak in November. This cyclical behavior is expected, as  $\Omega_{arag}$  and pH are directly and indirectly dependent on periodic values (surface  $pCO_2$  and temperature).

### 3.2 Population Dynamics Models



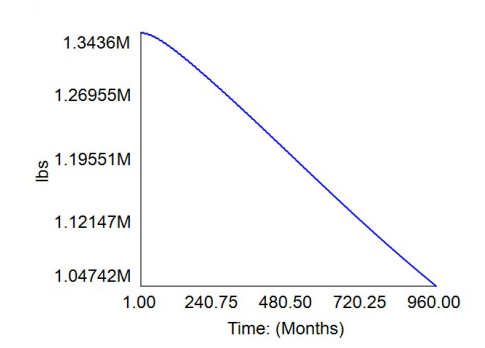
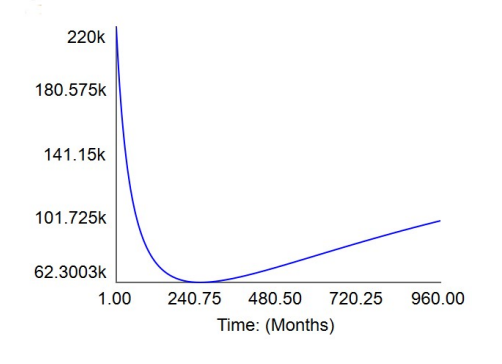


Figure 12: Pacific Oyster Larvae Stock

Figure 13: Pacific Oyster Harvest Weight

Figure 12 depicts the C. Gigas larvae stock at any given time. Values are displayed in thousands of individual larvae units. Figure 13 depicts the C. Gigas net harvest weight (lbs) at any given point.



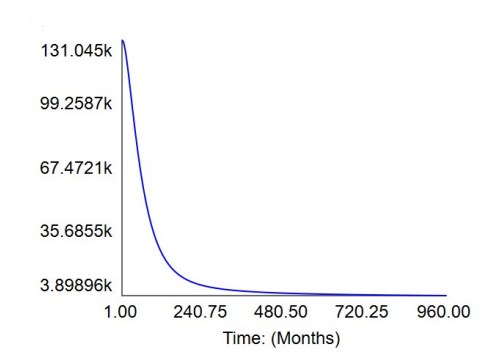


Figure 14: Geoduck D-Hinge Larvae Stock

Figure 15: Geoduck Dissoconch Stock

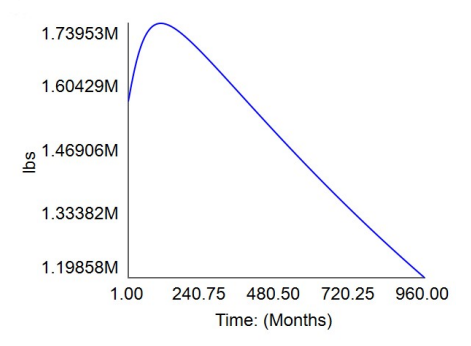
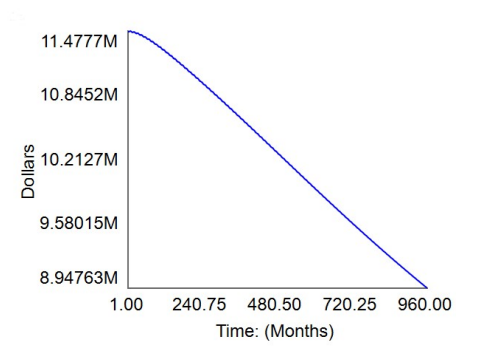


Figure 16: Geoduck Harvest Weight

Figure 14 depicts the P. Generosa d-hinge larval stock at any given point. Figure 15 depicts the P. Generosa dissoconch stock at any given time. Both values are displayed in thousands of individual larvae units. Figure 16 depicts P. Generosa the net harvest weight (lbs) at any given point.

# 3.3 Economical Dynamics Models



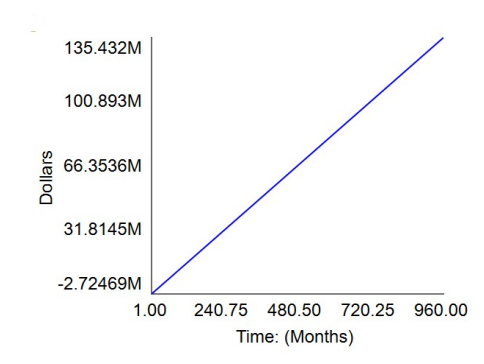
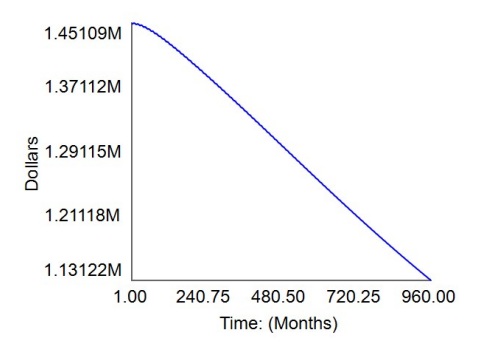


Figure 17: Pacific Oyster Harvest Net Annual Income Figure 18: Pacific Oyster Harvest Net Income Loss

Figure 17 depicts the net annual income (\$) from the C. Gigas harvest stock at any given time. Figure 18 depicts the accumulated income loss (\$) due to C. Gigas harvesting change for the South Puget Sound shellfish industry over an 80-year period.



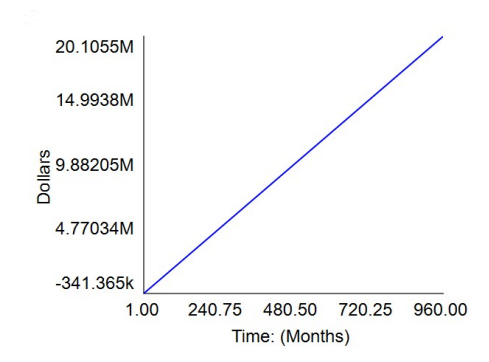
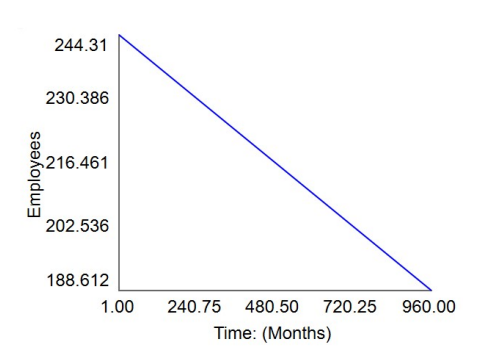


Figure 19: Pacific Oyster Harvest Net Annual Profit Figure 20: Pacific Oyster Harvest Net Profit Loss

Figure 19 depicts the net annual profit (\$) from the C. Gigas harvest stock at any given time. Figure 20 depicts the accumulated profit loss (\$) due to C. Gigas harvesting change for the South Puget Sound shellfish industry over an 80-year period.



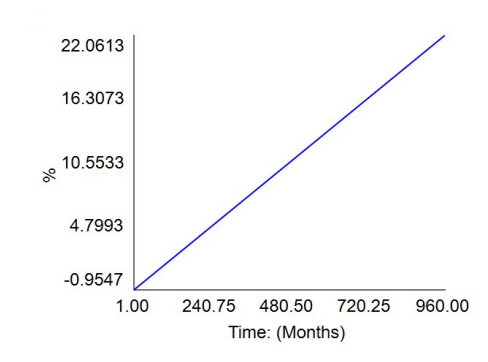
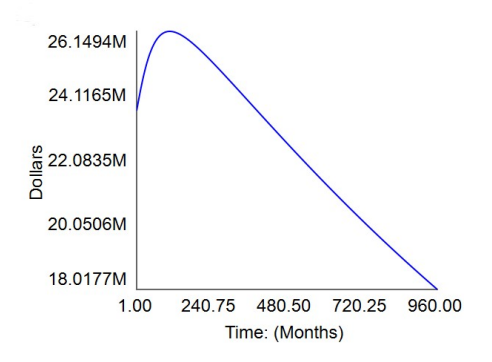


Figure 21: Pacific Oyster Harvesting Jobs

Figure 22: Percent Pacific Oyster Harvesting Jobs Lost

Figure 21 depicts the number of jobs directly related to harvesting C. Gigas at any given time. Figure 22 depicts the percentage of C. Gigas harvesting jobs lost from initial over an 80-year period.



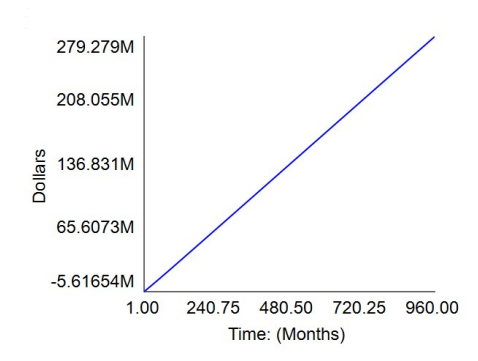
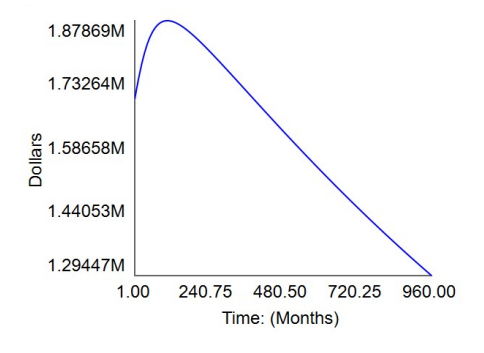


Figure 23: Geoduck Harvest Net Annual Income

Figure 24: Geoduck Harvest Net Income Loss

Figure 23 depicts the net annual income (\$) from the P. Generosa harvest stock at any given time. Figure 24 depicts the accumulated income loss (\$) due to P. Generosa harvesting change for the South Puget Sound shellfish industry over an 80-year period.



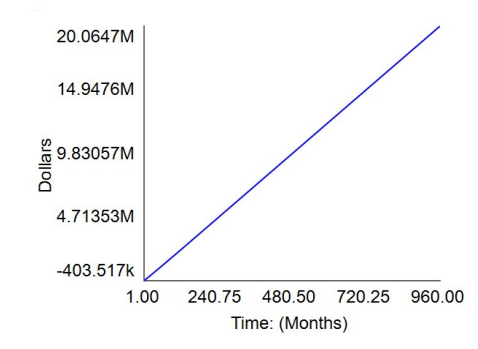
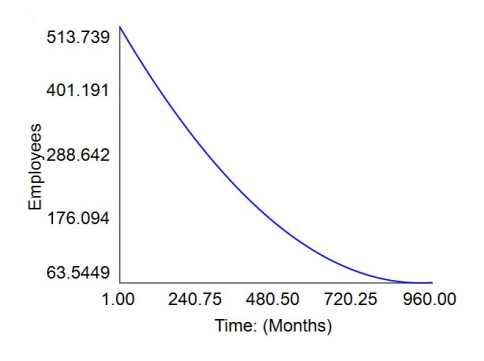


Figure 25: Geoduck Harvest Net Annual Profit

Figure 26: Geoduck Harvest Net Profit Loss

Figure 25 depicts the net annual profit (\$) from the P. Generosa harvest stock at any given time. Figure 26 depicts the accumulated profit loss (\$) due to P. Generosa harvesting change for the South Puget Sound shellfish industry over an 80-year period.



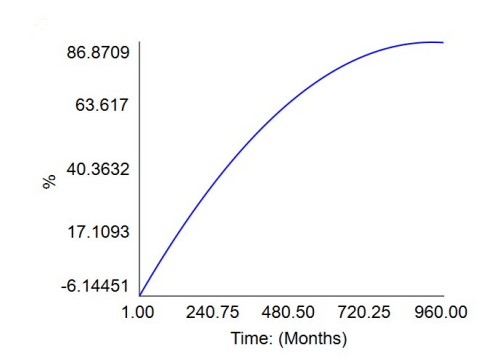


Figure 27: Geoduck Harvesting Jobs

Figure 28: Percent Geoduck Harvesting Jobs Lost

Figure 27 depicts the number of jobs directly related to harvesting P. Generosa at any given time. Figure 28 depicts the percentage of P. Generosa harvesting jobs lost from initial over an 80-year period.

#### 4. Discussion and Conclusion

### 4.1 Aquatic Chemistry Model

The results of the sinusoidal atmospheric  $CO_2$  input model result in atmospheric  $pCO_2$  levels nearly identical to the IPCC A1F1 climate scenario. After factoring in upwelling and atmospheric flux, we predict the South Puget Sound surface  $pCO_2$  levels will drop from an initial value of 560 ppm to a minimum of 553 ppm. After this initial drop, we estimate that surface  $pCO_2$  will rise exponentially to 735 ppm by the end of the century. The initial drop in  $pCO_2$  is expected, given that South Puget Sound's waters are currently more  $CO_2$  saturated than the atmosphere. However, we found that anthropogenic atmospheric inputs will reverse this relationship in approximately 14 years.

We also found that pH will drop by around 0.16 over the next 80-year period. The estimated current value of pH was 8.18, which is fairly close to global averages. pH seems to follow an inverse relationship with  $pCO_2$ . As  $pCO_2$  initially drops, pH increases slightly. When  $pCO_2$  begins to increase exponentially, pH drops exponentially. This behavior is also expected, as all other variables are either held as constant or vary annually. The implications of these results are numerous, as  $CO_2$  behavior directly affects pH and indirectly affects related significant values.  $\Omega_{arag}$  follows a similar pattern to pH, with an initial value of 0.525 and a final value of 0.149 (a drop of 0.376). However, the predicted decoupling behavior between pH and  $\Omega_{arag}$  is also apparent.  $\Omega_{arag}$  decreases at a rate higher than that of pH, and seasonal variation is far more significant. This is due to added variables in the  $\Omega_{arag}$  calculation that are directly related to temperature, further compounding its significance.

#### 4.2 Population Dynamics Models

Our model predicts that the Pacific Oyster larvae stock will drop from an initial of 220,000 units to approximately 186,000 units (a difference of 34,000 units). For the first 40-year period, the stock displays logarithmic decay behavior. After reaching a minimum unit stock of 184,093 units, the stock proceeds to rise logarithmically to a maximum of 187,000 units. It is interesting to note that, of all population values, only the C. Gigas larvae stock displayed a high sensitivity to seasonal temperature fluctuations. This is likely because the growth rate function relating  $\Omega_{arag}$  to C. Gigas larval development retains the  $\Omega_{arag}$ -temperature relationship. The Pacific Oyster harvest weight is also predicted to drop from an initial 1,343,600 lbs to a final value of 1,047,420 lbs (a difference of 296,180 lbs). Unlike the fluctuating rate of change present with the larvae stock, the harvest weight drops at a relatively linear rate. The harvest weight displays a slight sensitivity to temperature fluctuations, but not as significant as the larval stock sensitivity.

We also predict that the Geoduck d-hinge larvae stock will drop rapidly in the first 20 years, from an initial of 220,000 units to approximately 62,300 units. It will then begin rising at a fairly linear rate till the year 2100. The P. Generosa dissoconch stock is also predicted to drop, from an initial of 131,045 units to a final of approximately 3,899 units. The rate of logarithmic decay is extremely high for the first 8-10 years, resembling a linear relationship. We found that the Geoduck annual harvest weight will increase from an initial of 1.57 million lbs to a maximum of 1.74 million lbs by 2030. It will then decrease at a fairly linear rate to approximately 1.2 million lbs. None of the Geoduck population values display any sensitivity to seasonal temperature variation. This is likely due to the different dependency variables between C. Gigas and P. Generosa mid-stage growth rates. C. Gigas growth is dependent on  $\Omega_{arag}$ , while P. Generosa growth is dependent on pH. pH does not display the same degree of sensitivity to temperature variation as  $\Omega_{arag}$ .

Our results show that all population values for the Pacific Oyster and Geoduck will decrease significantly by 2100. The degree of annual harvest decay is greater for Geoducks when compared to Pacific Oyster annual harvest decay. This behavior is expected, given that ocean acidification affects Geoducks in the larval stage, while it only affects Pacific Oysters post early-stage growth. It is important to note that harvests are not continuously occurring, but are rather averaged over each 12-month interval (considered the "annual" harvest). This population model illustrates how devastating ocean acidification can be to calcifying organisms, as shown by the growth disparity between "protected" larvae in harvesting centers and "wild" larvae.

### 4.3 Economical Dynamics Models

We estimate the net annual income from the Pacific Oyster harvest will drop at a fairly linear rate, from an initial of \$11.48 million to \$8.95 million. The accumulated income loss rises linearly as a consequence. The initial income loss is \$-2.72 million (a \$2.72 million income gain) since the harvest values increase in the first few years. By 2100, the net predicted income loss for the South Puget Sound community is \$135 million due to the effects of OA on Pacific Oysters. However, this figure did not factor in labor and harvesting costs. To gain a more accurate picture of the net value Pacific Oyster's provide to the South Puget Sound

community, we analyzed the net profit loss. We predict that net annual profit from Pacific Oyster harvesting will decrease linearly from \$1.45 million to \$1.13 million by 2100.

We estimated the net annual income from the Geoduck harvest will rise from an initial of \$23.6 million to a maximum of \$26.1 million. Annual income drops at a fairly linear rate to a final value of approximately \$18 million. The accumulated income loss then rises linearly. Initial income loss is \$-5.62 million. By 2100, the net predicted income loss for the South Puget Sound community is \$279 million due to the effects of OA on Geoduck larvae. We predict that net annual profit from Geoduck harvesting will increase initially from \$1.7 million to \$1.88 million by 2030. It will then decrease to \$1.29 million. For both species affected by ocean acidification, the accumulated profit loss model predicts that the South Puget Sound economy will lose \$40.2 million dollars over the century.

The predicted number of jobs directly related to Pacific Oyster harvesting drops from 244 to 189, or a loss of 55 employees. By itself, the number of employees lost is not excessive over a near-century scale. However, the proportion of jobs lost by 2100 is approximately 22.1%. The predicted number of jobs directly related to Geoduck harvesting drops from 514 to 62. This corresponds to an 86.7% proportion of jobs lost. Other regional industries dependent on Pacific Oyster and Geoduck harvesting, such as packaging, transportation, hospitality, etc., may be affected in similar ways, if not to the same degree.

#### 4.4 Model Limitations and Future Research

The most significant limitation for this model was a lack of sufficient experimental data regarding the effects of  $\Omega_{arag}$  on C. Gigas and P. Generosa mid-stage and larval-stage growth. However, we were able to approximate larval growth for Geoducks and mid-stage growth for Pacific Oysters with a relative degree of accuracy through parameter estimation. The lack of previous research on mortality rate, birth rate, and Geoduck early-stage growth rate meant that we used estimated constants. While this did not significantly affect Pacific Oyster yields, it was much more apparent in the Geoduck model. Harvest values behaved in a reasonable manner, but dissoconch stage and d-hinge larvae stocks decreased rapidly before either flattening or increasing. This rapid decrease in population does not have an experimental justification. Rather, it is a consequence of holding certain flow rates constant while others are variable.

We also made assumptions regarding key values within the aquatic chemistry model. We held salinity, and by extension alkalinity, to be constant. This assumption was made since rainfall is a significant factor in measuring both salinity and alkalinity (Zhang, 2002). Unfortunately, regional rainfall predictions are hard to predict, further complicated by anthropogenic climate change. Similarly, we assumed temperature to be annually constant but seasonally varying in order to avoid compounding inaccuracies from global warming predictions. The sinusoidal upwelling rate generated from experimental  $pCO_2$  peaks is also a significant limitation. As evidenced by the 2007 upwelling event on the Washington State coast,  $CO_2$  rich water often results in sudden mortality events as opposed to slow changes in population. This model serves as a guide to average populations over time, but does not predict when significant mortality events will occur. Integrating separate models that predict temporal variability for temperature as well as alkalinity

will be key to making more accurate predictions. Other assumptions include constant surface wind speed, resulting in more stable atmospheric-marine flux behavior, as well as an approximation that  $C_{Alk}$  is 97.7% of Alkalinity at all times. To account for marine organism  $CO_2$  respiration, largely the cause of high deep ocean  $pCO_2$  levels, further study is required to determine how significant anthropogenic emissions are to acidification in South Puget Sound.

The economics model is relatively straightforward in its approach, but one significant assumption was that job losses correlated directly with income loss. This relationship is realistic for general behavior, since a decreasing net income results in fewer jobs (Sverker, 2018). The largest inaccuracy was a lack of layoff rates for workers, which was not considered due to a lack of experimental data. Generally, companies lay off lower level employees before senior executives, resulting in an sigmoid (s-shaped) loss relationship relative to the total number of employees and the number laid off (Federal Reserve St. Louis). This model does not take into account the larger economic impacts on recreational shellfish farmers in South Puget Sound due to a lack of experimental data. It also does not account for automation and technological changes. Future studies will have to integrate the impact of changing shellfish populations on individual farmers in addition to commercial harvesting companies. To study the adverse effects of OA on socioeconomic disparities in South Puget Sound, we will need to relate social demographic variables to the economics model. These additions are necessary to gain a better understanding of how significant the impacts of ocean acidification will be on individual communities, but are currently limited due to insufficient data.

## 4.5 Potential Solutions

Future research will also have to be conducted regarding solutions to the various environmental, ecological, and economic issues identified by this study. The most obvious solution to these issues is to reduce  $CO_2$  emissions on a global scale. As shown by this study, increases in atmospheric  $CO_2$  are significant for both surface and deep ocean water  $pCO_2$  levels. While acidity changes would be drastically reduced by this change, it is unrealistic to expect that all  $CO_2$  emissions could be phased out in such a short period of time. Even if this was a possibility, ocean acidification would continue for a certain period of time, as planetary systems react to atmospheric changes in a differential manner (Hansen et. al., 2007). However, reducing  $CO_2$  emissions over a reasonable period of time is still a necessity to combat the numerous consequences of ocean acidification and climate change. In recent years, land-based aquaculture has been proposed as a solution to many issues caused my marine aquaculture (Poppick, 2018) (Oliveira et al., 2020), including susceptibility to parasites and infections, sedimentation regulation, as well as acidification. This study shows that shellfish larvae and adult populations will both be adversely affected by acidification, and land-based aquaculture may be a viable option to pursue whether or not communities have easy access to marine and estuarine waters.

To address the socioeconomic consequences of acidity change, it is important to consider the particular issues at hand. Job and income loss do not necessarily reflect the economic success of a particular community, but are only estimates relative to its current state. While issues related to job loss, such as automation, artificial intelligence, and labor outsourcing (Estlund, 2018) are beyond the scope of this study, a few potential solutions are apparent. If acidification and its ecological consequences are to occur, alternative employment opportunities for affected farmers could be put in place as a mitigation technique. These employment opportunities could range from investment in job training to new market and job creation (Estlund, 2018). While the ideal solution to economic and social changes is a subject of great debate, this study makes it clear that effective solutions must be explored.

#### 4.6 Final Conclusion

When considering the effects of ocean acidification and related phenomena, researchers and scientists often emphasize the environmental impacts of climate change. While these are significant, it is also important to focus on lasting societal impacts of climate change, impacts which are heavily integrated with those same environmental and ecological changes. It is clear that coastal communities will experience the worst effects of ocean acidification, as they depend on marine and estuarine waters for both nourishment and economic sustenance. The aim of this study was to predict the effects that ocean acidification will have on two key shellfish species and the economic condition of a single community using a three-step systems-dynamics model. The results of the aquatic chemistry model clearly show that acidification is occurring, as evidenced by a drop in both pH and  $\Omega_{arag}$  directly correlated with an increase in dissolved  $CO_2$  levels. The population dynamics models illustrate how both Pacific Oyster and Geoduck harvests will decrease significantly by 2100. The economics model then analyzes the effects of these changes, predicting that the South Puget Sound community will lose approximately \$40 million in profit and over 500 jobs by the end of the century. Given that this is a case study on a single community with only two species, ocean acidification is clearly shown to have profound effects on the economic viability of coastal communities. This study illustrates the link between rising  $CO_2$  levels and decreasing economic viability of the fishing industry, providing an avenue for future studies to explore the relationship between geochemical, ecological, and economic factors. It also emphasizes the importance of lowering anthropogenic  $CO_2$  emissions, mitigating lowered shellfish growth by isolating aquaculture tanks from marine waters, and providing alternative employment opportunities for farmers affected by acidification.

#### Works Cited

- [1] Ecological Research, Approaches for general rules of biodiversity patterns in space and time, https://esj-journals.onlinelibrary.wiley.com/journal/14401703
- [2] Ford, Andrew. Modeling the Environment. London: IslandPress, 2010.
- [3] Busch, D. Shallin; McElhany, Paul. Estimates of the Direct Effect of Seawater pH on the Survival Rate of Species Groups in the California Current Ecosystem. Washington: Stony Brook, 2016.
- [4] Murray, James W. et al. An inland sea high nitrate-low chlorophyll (HNLC) region with naturally high pCO2. Washington: Limnology and Oceanography, 2015.
- [5] Carbon Dioxide: Projected emissions and concentrations. 2015.
- [6] Decadal water-property trends in the California Undercurrent, with implications for ocean acidification, Meinvielle, M. and Johnson, Gregory C., JOURNAL OF GEOPHYSICAL RESEARCH: OCEANS, 2013.
- [7] Decadal variations in the California Current upwelling cells, K. Chhak, E. Di Lorenzo, GEOPHYSICAL RESEARCH LETTERS, 2007.
- [8] Seasonal and interannual oxygen variability on the Washington and Oregon continental shelves, S. A. Siedlecki, N. S. Banas, JOURNAL OF GEOPHYSICAL RESEARCH: OCEANS, 2014.
- [9] Experiments with Seasonal Forecasts of ocean conditions for the Northern region of the California Current upwelling system, Samantha A. Siedlecki, Isaac C. Kaplan, Scientific Reports, 2016.
- [10] Review of the West Coast Commercial Fishing Industry in 2004, Pacific States Marine Fisheries Commission, 2006.
- [11] Shellfish Aquaculture in Washington State, Final Report to the Washington State Legislature, 2015.
- [12] Exploring perceptions and experiences of the U.S. West Coast shellfish industry dealing with ocean acidification, Mabardy R., 2014.
- [13] Sensitivity of the regional ocean acidification and carbonate system in Puget Sound to ocean and freshwater inputs, Bianucci, L. et al., 2018.
- [14] Linking the biological impacts of ocean acidification on oysters to changes in ecosystem services: A review, Lemasson A. et al., 2017.
- [15] Trophic transfer of paralytic shellfish toxin (PST): Physiological and reproductive effects in the carnivorous gastropod Acanthina monodon, P. Andrade-Villagrán et al., Aquatic Toxicology, 2019.

- [16] The Pacific oyster, Crassostrea gigas, shows negative correlation to naturally elevated carbon dioxide levels: Implications for near-term ocean acidification effects, Barton, Alan et al., Limnology and Oceanography, 2012.
- [17] Oceanography Magazine: THE OFFICIAL MAGAZINE OF THE OCEANOGRAPHY SOCIETY, Barton, A et al., Oceanography, Volume 28, 2015.
- [18] Saturation-state sensitivity of marine bivalve larvae to ocean acidification, Waldbusser George, Hales Burke et al., Nature Climate Change, 2014.
- [19] Spatiotemporal variability and long-term trends of ocean acidification in the California Current System, Hauri C., Gruber N. et al., Biogeosciences, 2013.
- [20] A post-larval stage-based model of hard clam Mercenaria mercenaria development in response to multiple stressors: temperature and acidification severity, Miller Cale A., Waldbusser George G., Inter-Research, 2016.
- [21] Seagrass habitat metabolism increases short-term extremes and long-term offset of CO2 under future ocean acidification, Pacella Stephen R., Brown Cheryl A. et al., PNAS, 2018.
- [22] Evidence for Upwelling of Corrosive "Acidified" Water onto the Continental Shelf, Feely Richard A., Sabine Christopher L. et al., Science Magazine, 2008.
- [23] The combined effects of ocean acidification, mixing, and respiration on pH and carbonate saturation in an urbanized estuary., Feely Richard A., Alin Simone R. et al., Elsevier, 2010.
- [24] Does seawater acidification affect survival, growth and shell integrity in bivalve juveniles?, Bressnan M., Chinellato A., Munari M. et al., Elsevier, 2014.
- [25] Exploring perceptions and experiences of the u.s. west coast shellfish industry dealing with ocean acidification, Mabardy R., SeaGrant, 2014.
- [26] Timmins-Schiffman et. al., 2019, Timmins-Schiffman Emma et. al., Ecology and Evolution, 2019.
- [27] Potential impacts of ocean acidification on the Puget Sound food web, Busch D. Shallin et. al., ICES Journal of Marine Science, 2013.
- [28] Estimating Total Alkalinity in the Washington State Coastal Zone: Complexities and Surprising Utility for Ocean Acidification Research, Fassbender Andrea J. et. al., Estuaries and Coasts, 2016.
- [29] Impacts of Coastal Acidification on the Pacific Northwest Shellfish Industry and Adaptation Strategies Implemented in Response, Barton Alan et. al., Oceanography, 2015.
- [30] Determination of Alkalinity and Borate Concentration of Sea Water, Gast J.A., Thompson T.G. et. al., Analytical Chemistry, 1958.

- [31] Alkaline rains on the Tibetan Plateau and their implication for the original pH of natural rainfall, Zhang D. D. et. al., Journal of Geophysical Research: Atmospheres, 2002.
- [32] Societal causes of, and responses to, ocean acidification, Jagers Sverker C. et. al., Ambio, 2018.
- [33] Shellfish Hatcheries Adapt as Ocean Becomes More Acidic, Schreiber, Fisherman's Voice, 2018.
- [34] Ocean Acidification, Woods Hole Oceanographic Institution.
- [35] Geoduck, Washington Department of Fish and Wildlife.
- [36] Crassostrea Gigas, Food and Agriculture.
- [37] Panopea generosa, Evergreen Journal.
- [38] Pacific Oyster, Sea Grant.
- [39] Geoduck Clam, Alaska Department of Fish and Game.
- [40] The Provisions of Social Relationships and Adaptation to Stress, Weiss R., 1974.
- [41] Ocean Acidification Threatens Food Security, Report, Lemonick Michael D., 2012.
- [42] Layoffs and Discharges (Levels and Rates), Federal Reserve Bank of St. Louis.
- [43] Dabob, PMEL Carbon Program.
- [44] Global Ocean Acidification Explorer, PMEL Carbon Program.
- [45] IPCC The observational record, IPCC CO2 Records.
- [46] Why Does Atmospheric CO2 Peak in May?, Monroe Rob, Scripps Institution of Oceanography, 2013.
- [47] Ocean Acidification: Saturation State, National Oceanic and Atmospheric Association (NOAA).
- [48] The Rate of Air-Sea CO2 Exchange: Chemical Enhancement and Catalysis by Marine Microalgae, Matthews Ben.
- [49] Building Resilience in the Face of Ocean Acidification, U.S. Climate Resilience Toolkit.
- [50] Chemical Oceanography, Murray James W. (In preparation), Oxford Press.
- [51] The Future of Fish Farming May Be Indoors, Laura Poppick, Scientific American, 2018.
- [52] Aquaponics using a fish farm effluent shifts bacterial communities profile in halophytes rhizosphere and endosphere, Oliveira, V., Martins, P., et. al., Nature, 2020.
- [53] If we immediately stopped emitting greenhouses gases, would global warming stop?, Hansen, J., Sato, Mki. et. al., Earth Observatory at NASA, 2007.

- [54] What Should We Do After Work? Automation and Employment Law., Estlund Cynthia, The Yale Law Journal, 2018.
- [55] Ocean acidification: the other CO2 problem, Doney Scott C. et. al., Annual Review of Marine Science, 2009.
- [56] A cubic relationship between air-sea CO2 exchange and wind speed, Wanninkhof Rik et. al., Geophysical Research Letters, 1999.
- [57] What Should We Do After Work? Automation and Employment Law., Estlund Cynthia, The Yale Law Journal, 2018.